Walisongo Journal of Chemistry
Walisongo Journal of Chemistry Vol. 8 Issue 2 (2025), 292-305
ISSN: 2621-5985 (online); 2549-385X (print)
DOI: https://doi.org/10.21580/wjc.v8i2.28915

NaOH-MODIFIED ACTIVATED CARBON FROM CORNCOBS AS A HETEROGENEOUS CATALYST: SYNTHESIS AND APPLICATION IN ULTRASOUND-ENHANCED TRANSESTERIFICATION OF USED COOKING OIL

Rosanina Kartika Santana[1], Adilah Aliyatulmuna[1*], Nazriati[1], Amalia Qurrota A'yun[1]

[1]Department of Chemistry, Faculty of Mathematics and Natural Sciences, Universitas Negeri Malang

*Corresponding author: adilah.aliyatulmuna.fmipa@um.ac.id

Abstract

Biodiesel is an alternative fuel composed of fatty acid methyl esters that can be synthesized from renewable sources and offers lower combustion emissions compared to fossil fuels. In this study, biodiesel was produced via a transesterification reaction using a basic heterogeneous catalyst derived from corncob carbon, which was activated and surface-modified with NaOH to create active catalytic sites. XRD and FTIR analyses confirmed the presence of Na_2CO_3 and Na_2O, while SEM-EDX revealed a porous surface morphology with uniformly distributed sodium. Used cooking oil (UCO) served as the triglyceride source after undergoing degumming, neutralization, and adsorption processes to reduce free fatty acid (FFA) content. The transesterification reaction was conducted in an ultrasonic water bath using the reflux method at 60°C with an oil-to-methanol molar ratio of 1:12. The optimum reaction conditions were achieved using 0.5 wt% catalyst and a reaction time of 120 minutes, yielding 73.15% biodiesel. The quality of the biodiesel produced under optimum conditions was evaluated based on density, viscosity, acid value, and calorific value, which were 857 kg/m^3, 3.8743 cSt, 0.2504 mg KOH/g, and 11,168 cal/g, respectively. These values comply with the quality requirements specified in SNI 04-7182-2015. GC-MS analysis confirmed that the major components of the biodiesel were methyl oleate and methyl palmitate. The utilization of corncob waste as a sustainable catalyst support, combined with alkali modification and ultrasonic enhancement, offers improved catalytic efficiency under mild operating conditions. This eco-friendly catalyst demonstrates strong potential for green catalytic processes in renewable energy development.

Keywords: *Biodiesel, Used Cooking Oil, Corncobs, Activated Carbon, Catalyst*

Introduction

The global energy crisis and environmental degradation driven by fossil fuel consumption have intensified research into renewable alternatives, with biodiesel emerging as one of the most promising substitutes. As a highly populated nation, Indonesia faces continuously increasing energy demands, prompting the government to implement the Mandatory B35 program, which requires a 35%

Copyright © 2025 WJC | ISSN 2621-5985 (online) | ISSN 2549-385X (print)

biodiesel blend in diesel fuel (Wirawan et al., 2024). Although this policy reduces dependence on fossil fuels, the high production cost of biodiesel remains a major challenge due to the use of expensive feedstock and conventional catalysts. Used cooking oil (UCO) provides a low-cost and abundant alternative feedstock that also helps mitigate waste management issues (Rahman et al., 2025). However, UCO typically contains high level of free fatty acid (FFA > 2%) and polymerized compounds, necessitating pre-treatment and efficient catalytic systems to achieve optimum biodiesel yield (Monika et al., 2023).

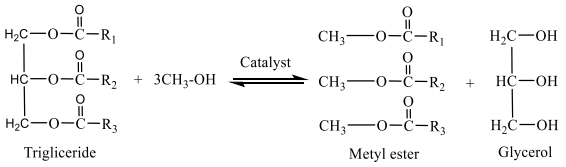

Figure 1. Transesterification reaction on triglycerides

The transesterification reaction converts triglycerides into fatty acid methyl esters (FAME) and glycerol through a reversible catalytic process involving short-chain alcohols (Naseef & Tulaimat, 2025). This reaction cannot proceed efficiently without a catalyst under mild conditions. Conventional homogeneous catalysts, however, present major drawbacks, including difficult separation, corrosiveness, and high water consumption, all of which elevate production costs and environmental impact (Mandari & Devarai, 2022). In contrast, heterogeneous catalysts offer a more sustainable option, with biomass-derived activated carbon gaining increasing attention due to its porous structure, stability, and cost-effectiveness (Nguyen et al., 2021).

Corncob, an agricultural by-product composed of 42–45% cellulose, is an excellent precursor for activated carbon (AC) because of its high carbon content and wide availability (Suminar et al., 2024). When modified with NaOH, the resulting catalyst forms active sites such as Na_2CO_3, which significantly enhance transesterification efficiency (Chana et al., 2025). Traditional catalyst synthesis methods typically require prolonged impregnation times (≥ 6 hours) and yield a basicity value of 7.03 mmol/g. In contrast, the present study introduces a NaOH-modified corncob-based catalyst synthesized through a more efficient activation and modification route. The combination of alkali modification and ultrasonic irradiation promotes the formation of basic active sites, improving catalytic activity during transesterification. This synergy also enhances mass transfer and surface interactions, resulting in higher catalytic efficiency and biodiesel yield under mild operating conditions.

Ultrasonication technology effectively addresses the mass transfer limitations commonly encountered during conventional stirring, thereby reducing reaction time and energy consumption. In this study, ultrasound-assisted impregnation was used to synthesize the NaOH-modified activated carbon catalyst from corncob, utilizing acoustic cavitation to rapidly and uniformly disperse active sites within a significantly shorter time compared to traditional methods (Hoo et al., 2022). Additionally, ultrasonic irradiation was applied during the transesterification process to improve interfacial contact between the immiscible oil and alcohol phases. The formation and collapse of microbubbles generate localized heating and micro-turbulence, which substantially enhance mass transfer and simultaneously lower the activation energy required for the reaction (Elgharbawy et al., 2024).

This study developed a sustainable and efficient heterogeneous catalyst derived from NaOH-modified corncob-activated carbon and evaluated its performance in the ultrasonic-assisted transesterification of UCO. This approach offers a promising pathway toward cost-effective and environmentally friendly biodiesel production.

Experimental Section

Materials

The materials used in this study included corncob-derived carbon (CC) from

Copyright © 2025 WJC | ISSN 2621-5985 (online) | ISSN 2549-385X (print)

Grobogan, Central Java; used cooking oil (UCO); distilled water; NaOH p.a. (Merck); KOH p.a. (Merck); 96% ethanol; 0.1 N $Na_2S_2O_3$ solution; 0.1 N iodine solution; 1% starch solution; toluene; 0.1 N HCl solution; 0.1 N $C_2H_2O_4$ solution; phenolphthalein indicator; bromothymol blue indicator; methanol; and anhydrous Na_2SO_4.

Instruments

The instruments used for measurement and characterization included a Scanning Electron Microscope (Carl Zeiss Evo MA 10), X-ray Diffraction (XRD) instrument (PANalytical X'Pert Pro), Fourier Transform Infrared (FTIR) spectrometer (Shimadzu IRPrestige 21), and Gas Chromatography–Mass Spectrometry (GC-MS) (Agilent 5977B).

Procedure

The use of UCO as a raw material for biodiesel production involved several stages: purification of UCO via degumming, neutralization, and adsorption using corncob-activated carbon with 5% KOH (CAC5) as the adsorbent; synthesis and characterization of the catalyst derived from corncob-activated carbon with 30% KOH, followed by modification using 35% NaOH (Na/CAC catalyst); ultrasound-assisted transesterification; and characterization of biodiesel properties, including density, viscosity, acid value, and calorific value.

Purification of Used Cooking Oil

UCO purification was performed through a three-stage process consisting of degumming, neutralization, and adsorption. In the degumming step, UCO was mixed with water at a 1:1 ratio, heated at 110°C, and stirred at 700 rpm until half of the water had evaporated. The mixture was then allowed to settle for 1 hour and subsequently filtered to remove gums.

The neutralization step involved treating 100 mL of degummed oil with 5 mL of 15% NaOH solution at 40°C for 10 minutes at 500 rpm. The mixture was then centrifuged to separate the neutralized oil from the soapstock (Hendi et al., 2021).

In the final stage, adsorption was carried out using CAC5, prepared by chemically activating CC with 5% KOH solution for 4 hours, followed by washing, drying at 110°C, and calcination at 400°C (Helwani et al., 2021). A total of 20 mL of neutralized oil was mixed with 0.02 g of CAC5 and shaken at 170 rpm for 60 minutes, followed by filtration to obtain purified used cooking oil (PUCO). PUCO was then analyzed for moisture content and free fatty acid (FFA) content.

Synthesis of Na/CAC Catalyst

CC was activated to increase its surface area. *First*, 20 g of CC was mixed with 200 mL of 30% KOH solution and stirred at 700 rpm for 4 hours using a magnetic stirrer. The mixture was filtered and dried at 110°C for 2 hours, followed by calcination at 400°C for 2 hours. The activated carbon was then washed until neutral pH and oven-dried at 80°C for 24 hours. The resulting material was designated as CAC30. The quality of CAC30 was assessed through moisture content and iodine number analysis, and its functional groups were characterized using FTIR.

For surface modification, 5 g of CAC30 was impregnated with 50 mL of 35% NaOH solution in an ultrasonic water bath for 150 minutes. The mixture was filtered, dried at 110°C, and calcined at 500°C for 4 hours (Chana et al., 2025). The final catalyst, referred to as Na/CAC, was analyzed for basic site concentration and characterized using XRD, FTIR, and SEM-EDX. The percentage of active sites on the catalyst surface was further determined using the MAUD (Material Analysis Using Diffraction) application.

The basic strength of the Na/CAC catalyst was evaluated using toluene and suitable indicators. Bromothymol blue (H_- = 7.2) turned blue, and phenolphthalein (H_- = 9.3) turned pink, indicating the basic strength range. Basicity was determined by titration, where approximately 0.05 g of the Na/CAC catalyst was mixed with 5 mL of toluene and phenolphthalein indicator, followed by titration with 0.1 N $H_2C_2O_4$.

Copyright © 2025 WJC | ISSN 2621-5985 (online) | ISSN 2549-385X (print)

$$Basicity\ (mmol/g) = \frac{V\ (mL) \times N\ (N)}{m\ (g)}$$

Application of Na/CAC Catalyst for Biodiesel Production

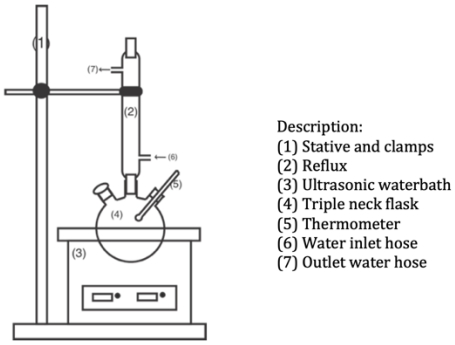

Figure 2. Ultrasonic-Assisted Transesterification Device Setup

The transesterification reaction was conducted using PUCO and methanol at a molar ratio of 1:12, with Na/CAC catalyst added at loadings of 0.5%, 2.5%, and 5% (wt%). The reaction was carried out in a three-neck flask placed in an ultrasonic bath operating at 40 kHz and 60°C, with reaction durations of 60, 90, and 120 minutes (Ansori & Mahfud, 2021).

After the reaction, the mixture was centrifuged to separate the catalyst. The upper biodiesel layer was decanted from the lower glycerol–methanol layer, then washed with hot distilled water at 50°C until the wash water became neutral. The biodiesel was dried with anhydrous Na_2SO_4 and filtered, followed by heating at 100°C for 15 minutes to remove residual moisture. The biodiesel yield was calculated, and fuel properties, including density, viscosity, acid number, and calorific value, were analyzed. Biodiesel characterization was performed using FTIR and GC-MS. To ensure statistical reliability, all experiments were carried out in duplicate, and the average values were reported.

The biodiesel yield was determined by weighing the final biodiesel product. The percentage yield was calculated using the following formula:

$$Yield = \frac{Biodiesel\ mass\ (g)}{Oil\ mass\ (g)} \times 100\%$$

Density was measured using a pycnometer. The empty pycnometer was weighed, then filled with biodiesel at 40°C and weighed again. Density was calculated as:

$$\rho = \frac{(W_2\ (g) - W_1(g))}{V\ (mL)}$$

Viscosity was measured using an Ostwald viscometer. The biodiesel sample was maintained at 40°C and allowed to flow through the viscometer placed in a thermostatic bath. Flow time was recorded, and viscosity was calculated using the following formulas:

$$\mu_{sample} = \frac{t_{sample} \times \rho_{sample}}{t_{water} \times \rho_{water}} \times \eta_{water}$$

$$vk = \frac{\eta_{sample}}{\rho_{sample}}$$

Acid number was measured by mixing 2 mL of biodiesel sample with 2 mL of 95% ethanol and adding three drops of phenolphthalein indicator. The solution was titrated with 0.1 N KOH until a persistent pink color appeared. Acid value was calculated using the formula:

$$Acid\ value = \frac{V_{KOH} \times N_{KOH} \times Mr_{KOH}}{m_{sample}}$$

The calorific value of the biodiesel was measured using a Parr Adiabatic Bomb Calorimeter. After combustion, the bomb was carefully vented and rinsed with distilled water. The rinsing solution and ignition wire residues were titrated with 0.0725 N Na_2CO_3 using methyl red indicator to determine correction factors for nitric acid formation and ignition wire combustion. The calorific value was then calculated based on the observed temperature rise, the calorimeter heat capacity, and the correction factors obtained from titration.

Results and Discussion

Purification of Used Cooking Oil

In a one-step transesterification process, UCO must contain less than 1% FFA to avoid saponification and ensure high biodiesel yield (Siang et al., 2024). The UCO used in this study was obtained from chicken frying at Warung Ayam Bu Oki in Jimbaran, which had undergone 4–5 frying

Copyright © 2025 WJC | ISSN 2621-5985 (online) | ISSN 2549-385X (print)

cycles. Purification was performed in three stages: degumming, neutralization, and adsorption using CAC5. This pretreatment method offers the advantage of minimizing oil loss during purification (Gharby, 2022).

Figure 3. The separation during the degumming stage

UCO from chicken frying typically contains protein residues, which are removed during degumming. The method applied in this study was water degumming, where hot water hydrates phospholipids. Once hydrated, these phospholipids become insoluble in oil and form a solid suspension at the bottom layer. The mixture was then separated using a separatory funnel, producing two distinct layers, as shown in **Figure 3**. After this step, the oil color changed from dark brown to a clearer brown.

Figure 4. The separation during the neutralization stage

Neutralization aims to reduce FFA and eliminate other undesirable compounds. In this process, the acidic hydrogen (H^+) from FFA reacts with hydroxide ions (OH^-) from NaOH to form soap and water (Kosma et al., 2025). After this stage, the oil turned yellow, as shown in **Figure 4**. The reaction is as follows:

$$\text{R-COOH}(l) + \text{NaOH}(aq) \rightarrow \text{R-COONa}(s) + \text{H}_2\text{O}(l)$$

Adsorption occurred through interactions between hydroxyl groups in the cellulose structure of CAC5 and the remaining FFA. The CC precursor was chemically activated using a 5% KOH solution. Potassium and hydroxide ions penetrated the carbon matrix and participated in reactions during thermal activation, forming pores within the carbon structure. The quality of CAC5 was evaluated according to the Indonesian Standard SNI 06-3730-1995, with the results shown in **Table 1**.

(a) (b)

Figure 5. (a) UCO (b) PUCO

After the purification stages, the oil changed to a yellow color, as illustrated in **Figure 5**. The PUCO was subsequently analyzed for moisture content and FFA content, which are presented in **Table 2**. Based on these results, the purification process successfully reduced the FFA level to below 1%, indicating that PUCO is suitable for direct transesterification without requiring a prior esterification step.

Synthesis of Na/CAC Catalyst

In the synthesis of the Na/CAC catalyst, CAC30 served as the catalyst support, providing a porous structure for the dispersion of active sites. The physicochemical properties of CAC30, which determined its effectiveness as a support material, are presented in **Table 3**.

Copyright © 2025 WJC | ISSN 2621-5985 (online) | ISSN 2549-385X (print)

Table 1. Comparison of CC and CAC5 quality

Parameter	CC	CAC5	SNI 06-3730-1995
Moisture Content (%)	3.983	1.754	Max. 15%
Iodine Number (mg/g)	734.204	925.849	Min. 750 mg/g

Table 2. Comparison of UCO and PUCO quality

Parameter	UCO	PUCO	SNI 01-3741-2002
FFA Content (%)	1.688	0.242	Max. 0.30%
Moisture Content (%)	2.032	0.076	Max. 0.30%

Table 3. Physicochemical properties of CAC30

Parameter	CAC30	SNI 06-3730-1995
Moisture Content	2.698%	Max 15%
Iodine Number	974.632 mg/g	Min 750 mg/g

As reported in the authors' previous study (currently under revision), surface area analysis using the full BET isotherm for 5% KOH-activated carbon yielded 674.194 m^2/g. In the present work, 30% KOH was used as the activating agent. According to Al-Swaidan and Ahmad (2011), the specific surface area of activated carbons generally increases with higher concentrations of chemical activators. A larger surface area supports more uniform dispersion of metal or alkali species, while abundant oxygen-containing functional groups enhance metal–support interactions and promote the formation of active catalytic sites.

FTIR analysis of CAC30 as catalyst support

FTIR analysis revealed a broad peak at 3399 cm^{-1} for CC and 3395 cm^{-1} for CAC30, indicating the presence of adsorbed water molecules within the carbon structure. Absorption bands at 2919 cm^{-1} and 2923 cm^{-1} correspond to aliphatic C–H stretching vibrations of CH_3 and CH_2 groups. Peaks at 1686 cm^{-1} and 1688 cm^{-1} indicate carbonyl (C=O) groups from carboxylic acids, which are characteristic of activated carbon. The polarity of C=O groups facilitates interaction with other molecules through van der Waals forces and hydrogen bonding (Hisbullah, 2022). Peaks for C=C functional groups appeared at 1597 cm^{-1} and 1568 cm^{-1}, while C–O stretching vibrations were observed at 1216 cm^{-1} and 1210 cm^{-1}. At these wavelengths, both C=C and C–O groups exhibited red shifts and increased intensity due to electron delocalization from K^+ ions into the aromatic system or the formation of C–O–K bonds.

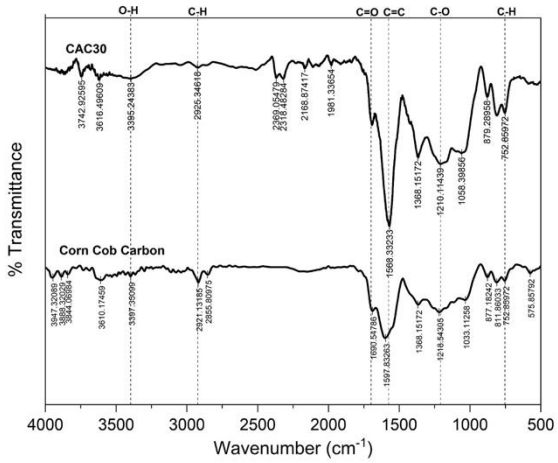

Figure 6. FTIR spectrum of CAC30 compared to CC

Copyright © 2025 WJC | ISSN 2621-5985 (online) | ISSN 2549-385X (print)

Figure 7. Na/CAC catalyst

CAC30 was then impregnated with NaOH, resulting in the formation of active sites on its surface. Successful synthesis of the Na/CAC catalyst was confirmed through characterization, which indicated the presence of Na_2CO_3 and Na_2O. The reaction occurring during NaOH incorporation into CAC30 at approximately 500°C is shown below (Nyepetsi et al., 2024):

$$4NaOH(aq) + C(s) \rightarrow Na_2CO_3(s) + Na_2O(s) + 2H_2(g)$$

The Na/CAC catalyst was evaluated for basic strength and surface basicity. The basicity of the active sites originates from oxygen atoms in the oxide compounds, which can donate lone electron pairs during the reaction. Testing the basic sites aims to determine their quantity and strength, both of which are closely related to catalytic performance. The measured basicity of the Na/CAC catalyst was 7.71 mmol/g, with a basic strength ranging from 9.8 to 15.0.

Analysis of XRD Pattern of Na/CAC Catalyst

The XRD pattern of the Na/CAC catalyst is presented in **Figure 8**. The characteristic peaks of Na_2CO_3 were observed at 2θ angles of 27.53°, 29.99°, 34.27°, 35.19°, 37.84°, 39.96°, 41.26°, 46.45°, 48.19°, and 53.49°, corresponding to the standard Na_2CO_3 peaks from COD 9011304. The formation of Na_2O active sites was also identified at 2θ angles of 32.34° and 46.45°, which match the standard Na_2O peaks from COD 9009063. The sharp and well-defined peaks indicate that both compounds are crystalline.

It is important to note that no distinct NaOH peak was detected, despite its extensive use during catalyst preparation. This suggests that Na_2CO_3 was the predominant compound present on the catalyst surface. Phase composition analysis using MAUD software confirmed that the synthesis of the Na/CAC catalyst resulted in Na_2CO_3 and Na_2O phases as the active sites, with respective proportions of 92.997% and 7.003%.

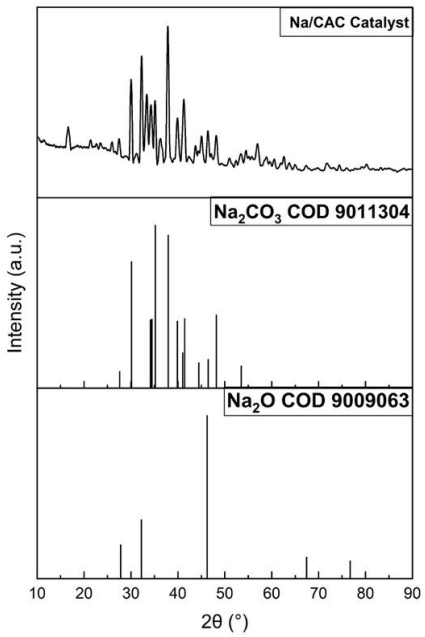

Figure 8. Diffractogram of Na/CAC catalyst

FTIR Analysis of Na/CAC Catalyst

The FTIR analysis of the Na/CAC catalyst, presented in **Figure 9**, revealed absorption bands characteristic of Na_2CO_3 formation. Peaks at 3715 cm^{-1} and 3850 cm^{-1} indicate the presence of hydroxyl groups associated with moisture adsorption. The peak at 2984 cm^{-1} corresponds to CH_2 vibrations of alkyl groups (Wang et al., 2020). The absorption at 2493 cm^{-1} represents C=O vibrations in calcite-like carbonates. The bands at 1446 cm^{-1} and 879 cm^{-1} correspond to the symmetric and asymmetric C–O stretching vibrations of carbonate groups, confirming the formation of Na_2CO_3 as active sites. In comparison, unmodified CAC30 displayed dominant C=C (1570 cm^{-1}) and C–O (1212 cm^{-1}) peaks. The modified catalyst, however, exhibited new carbonate-related bands, and the C=C peak was no longer

Copyright © 2025 WJC | ISSN 2621-5985 (online) | ISSN 2549-385X (print)
Volume 8, Nomor 2, 2025

visible due to overlap with stronger carbonate absorptions. These results confirm the successful formation of Na_2CO_3 following NaOH modification.

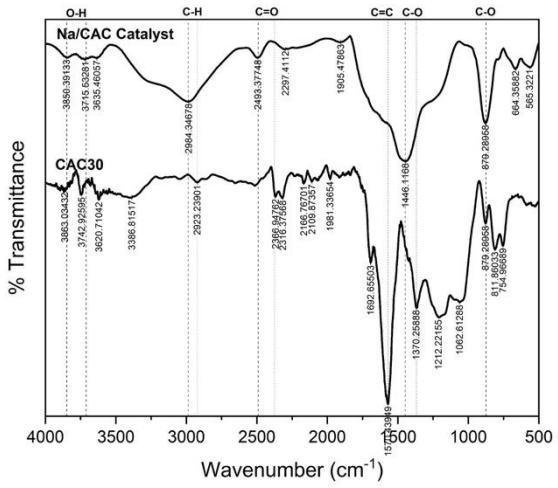

Figure 9. FTIR spectrum of Na/CAC catalyst compared to CAC30

Analysis of SEM-EDX of Na/CAC Catalyst

The surface morphology of the catalyst was examined using SEM, as shown in Figure 10. On the surface of CC (see **Figure 10a**), the structure appeared dense and irregular with few visible pores. After activation (see **Figure 10b**), the surface of CAC30 became more structured and displayed open pores, indicating that the activation process effectively widened pore walls and generated new pore structures. The modification of active sites on CAC30 (see **Figure 10c**) resulted in the appearance of dispersed particles on the carbon surface, which served as catalyst support.

Table 4. Elemental analysis of Na/CAC catalyst

Material	Element Content (wt%)			
	C	O	K	Na
CC	72.36	24.22	1.57	0.00
CAC30	78.76	18.75	1.86	0.00
Na/CAC	17.90	57.24	0.36	23.55

Based on the EDX results in **Table 4**, the carbon content increased from 72.36 wt% to 78.76 wt% after activation with 30% KOH due to the removal of impurities. However, a sharp decrease in carbon content was observed in the Na/CAC catalyst, dropping to 17.90 wt% as a result of the reaction between CAC30 and NaOH. This reaction produced new inorganic compounds such as Na_2CO_3 and Na_2O, which bind a portion of the carbon into non-carbonaceous phases, reducing the amount of free carbon detected by EDX. Additionally, the oxygen content increased from 18.75 wt% in CAC30 to 57.24 wt% in Na/CAC, while sodium, absent in CAC30, appeared at 23.55 wt% in Na/CAC, indicating successful NaOH impregnation into the CAC30 matrix. The increased sodium and oxygen content is likely associated with NaOH decomposition into hydroxyl (–OH) and carbonate (CO_3^{2-}) groups.

Characterization of the Na/CAC catalyst using XRD, FTIR, and SEM-EDX confirmed the successful activation and alkali modification of CC. XRD analysis showed peaks at 2θ values between 27° and 54°, validating the presence of Na_2CO_3 as an active catalytic phase. FTIR spectra exhibited characteristic absorption bands of carbonate species (Na_2CO_3) in the range of 1420–1460 cm^{-1}, indicating the formation of basic sites after NaOH modification. SEM-EDX analysis revealed the presence of sodium (23.55 wt%) after modification, confirming the incorporation of Na_2CO_3 species on the catalyst surface. Collectively, these results demonstrate that chemical activation and alkali modification successfully enhanced the structural, morphological, and chemical properties of the catalyst, increasing its basicity and catalytic performance for biodiesel synthesis.

Copyright © 2025 WJC | ISSN 2621-5985 (online) | ISSN 2549-385X (print)

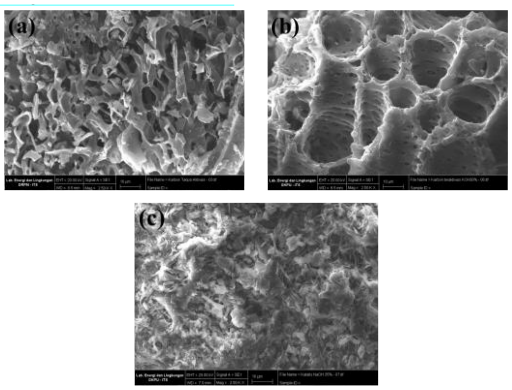

Figure 10. Morphology of (a) CC, (b) CAC30, and (c) Na/CAC catalysts

Application of Na/CAC Catalyst for Biodiesel Production

(a) (b) (c)

Figure 11. (a) UCO, (b) PUCO, and (c) biodiesel

The Na/CAC catalyst was applied to optimize biodiesel synthesis using UCO as the feedstock. The oil was first purified to reduce its FFA content to below 1%. Transesterification of PUCO was performed under fixed reaction conditions using the Na/CAC catalyst, with a PUCO-to-methanol molar ratio of 1:12, a reaction temperature of 60°C, and an ultrasonic frequency of 40 kHz. The effects of catalyst loading and reaction time on biodiesel yield were investigated in this study.

Effect of Na/CAC Catalyst and Reaction Time on Biodiesel Yield

The Na/CAC catalyst with various mass loadings (0.5%, 2.5%, and 5% (wt%)) was applied in the biodiesel synthesis from PUCO at different reaction times (60, 90, and 120 minutes). The biodiesel yield obtained from each transesterification reaction is presented in **Figure 12**.

Figure 12 shows that the highest biodiesel yield was achieved using a catalyst loading of 0.5% (wt%) with a reaction time of 120 minutes, reaching 73.15%. The biodiesel yield initially increased with the rise in catalyst loading from 0.5% to 5% (wt%), as a higher catalyst mass provides more active sites for the transesterification reaction (Yang et al., 2017). However, adding a catalyst beyond the optimum level can reduce biodiesel yield. This occurs due to the reversible nature of the transesterification reaction, where excess catalyst may promote reverse reactions that convert methyl esters back into triglycerides.

For basic catalysts, an excess of active sites can also trigger undesirable side reactions with residual FFAs, forming soap through saponification. Soap formation increases the viscosity of the reaction mixture and promotes emulsification, which disrupts the separation of glycerol and biodiesel layers, ultimately decreasing the yield (Larimi et al., 2024).

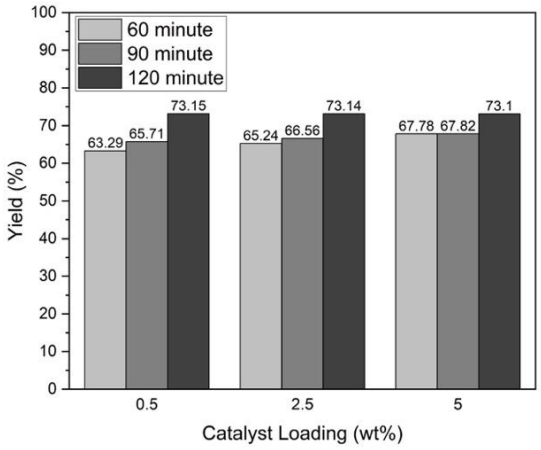

Figure 12. Biodiesel yield obtained using various Na/CAC catalyst loadings

Biodiesel yield also increased as the reaction time was extended from 60 to 120 minutes. However, at 120 minutes, the yield became relatively constant across all catalyst loadings, indicating that the reaction had reached equilibrium. At the early stages of the process, the mixing between alcohol and oil occurred gradually, but once sufficient contact was established, the reaction proceeded rapidly and reached its maximum yield.

Copyright © 2025 WJC | ISSN 2621-5985 (online) | ISSN 2549-385X (print)

Effect of Na/CAC Catalyst and Reaction Time on the Calorific Value of Biodiesel

Figure 13 shows that the highest biodiesel calorific value was produced using a catalyst loading of 0.5% (wt%) with a reaction time of 120 minutes, reaching 11,168 cal/g. A high calorific value indicates that a large amount of heat is released during combustion, which enhances engine performance. The calorific value of the synthesized biodiesel exceeded that of diesel fuel (10,270 cal/g), except for the condition using 5% catalyst loading and a 90-minute reaction time. Nonetheless, the calorific value under this condition still surpassed that of coal (9,314 cal/g).

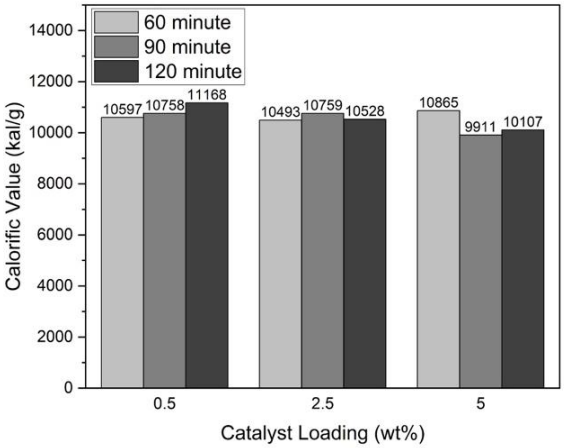

Figure 13. Calorific value of biodiesel produced using different Na/CAC catalyst loadings

Variations in catalyst loading and reaction time did not significantly affect the calorific value of biodiesel. This is because calorific value is primarily affected by the molecular characteristics of biodiesel, such as carbon chain length and the degree of fatty acid saturation (Tamilselvan et al., 2020). Biodiesel with a higher saturated fatty acid content typically exhibits a higher calorific value due to the greater energy stored in single C–C bonds, which is released during combustion.

FTIR Analysis of Biodiesel

The spectral characteristics of PUCO and biodiesel in **Figure 14** show that both contain identical chemical functional groups, as the transesterification reaction primarily involves the removal of glycerol and the substitution of a methyl group in the hydrocarbon chain (Alkinani et al., 2025). This confirms that FAME, like oil, retains structural elements such as CH_2 groups, C=C double bonds, C=O carbonyl groups, and C–O ester bonds.

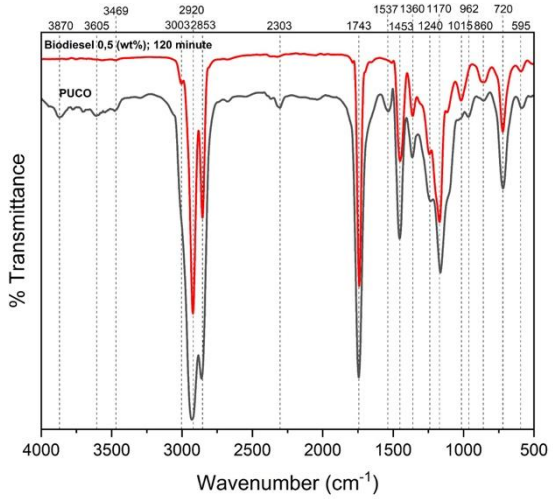

Figure 14. FTIR spectrum of biodiesel with 0.5% catalyst loading and 120-minute reaction time compared to PUCO

Table 5. FTIR spectra analysis of biodiesel

Wavenumber (cm^{-1})		Functional Group
PUCO	Biodiesel	
2925	2921	C-H alkanes
2860	2851	
1743	1739	C=O ester
1452	1452	C-H asymmetric
1164	1167	C-O stretching
862	856	C-H bending
719	721	C-H rocking

A significant difference between the two spectra appeared at the peak around 1014 cm^{-1} in the biodiesel spectrum, which was absent in the PUCO. This peak corresponds to the oscillation vibration of the (CH_3–O) group resulting from the deformation vibration of CH_3 in the ester group, indicating the successful conversion of oil into biodiesel (Kongto et al., 2022).

Meanwhile, peaks at 1537 cm^{-1} and 2303 cm^{-1}, observed only in the oil, are associated with C=C double bonds. Their absence in the biodiesel spectrum suggests

Copyright © 2025 WJC | ISSN 2621-5985 (online) | ISSN 2549-385X (print)

a reduction in chain length following the conversion process. The absorption around 3000 cm^{-1} in the oil indicates the presence of O–H groups, likely originating from residual FFAs in the purified oil. The disappearance of this peak in the biodiesel spectrum further confirms the conversion to methyl esters.

GC-MS Analysis of Biodiesel

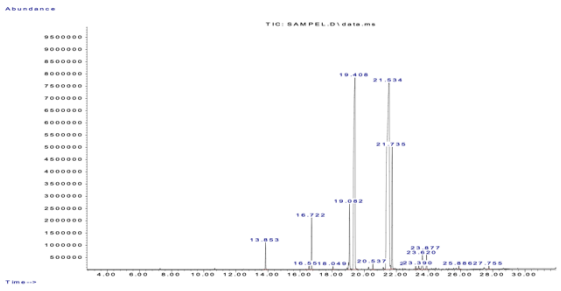

Figure 15. Chromatogram of biodiesel

Table 6. FAME composition of biodiesel with 0.5% catalyst loading and 120-minute reaction time

The GC-MS chromatogram of the biodiesel sample displayed several distinct peaks corresponding to FAME, the primary components of biodiesel. Major peaks observed at retention times around 19.4 and 19.5 minutes indicate the dominant presence of methyl oleate and methyl palmitate. Minor peaks at earlier retention times represent shorter-chain methyl esters or trace impurities. The high intensity of the main peaks demonstrates that the transesterification of UCO was successfully completed.

Table 6 shows that the most abundant compounds in biodiesel produced with 0.5% catalyst loading and a 120-minute reaction time were 9-octadecenoic acid (oleic acid) and hexadecanoic acid (palmitic acid). This composition is consistent with findings from previous studies using UCO as feedstock.

Table 7. FAME composition of biodiesel with 0.5% catalyst loading and 120-minute reaction time

Name of FAME	Retention Time	% Area
Dodecanoic acid, methyl ester	13.853	1.28
cis-9-Tetradecenoic acid, methyl ester	16.559	0.21
Tetradecanoic acid, methyl ester	16.722	2.52
Pentadecanoic acid, methyl ester	18.049	0.15
9-Hexadecenoic acid, methyl ester	19.082	3.95
Hexadecanoic acid, methyl ester	19.408	29.22
Heptadecanoic acid, methyl ester	20.537	0.28
9-Octadecenoic acid, methyl ester	21.534	51.42
Octadecanoic acid, methyl ester	21.735	8.00
5,8,11,14-Eicosatetraenoic acid, methyl ester, (all-Z)-	23.201	0. 22
Methyl dimethylhexadecadienoate (18:2)	23.390	0.33
cis-11-Eicosenoic acid, methyl ester	23.620	1.09
Eicosanoic acid, methyl ester	23.877	0.99
Docosanoic acid, methyl ester	25.886	0.17
Tetracosanoic acid, methyl ester	27.755	0.17

Physical Properties of Produced Biodiesel

Table 7 lists several biodiesel properties measured in this study and compares them with UCO, PUCO, and the SNI 7182-2015 standard. Several measured properties confirm that the synthesized biodiesel met the required specifications. These findings demonstrate the viability of the Na/CAC catalyst as a heterogeneous catalyst for biodiesel production from UCO.

Table 8. Physical properties of biodiesel with 0.5% catalyst loading and 120-minute reaction time

Material	Physical Property		
	Density (kg/m^3)	Viscosity (cSt)	Acid Number (mgKOH/g)
UCO	913.8	28.3677	3.6989
PUCO	917.8	29.2642	0.5308

Copyright © 2025 WJC | ISSN 2621-5985 (online) | ISSN 2549-385X (print)

Biodiesel	857.0	3.8743	0.2504
SNI 7182-2015	850-890	2.3-6.0	Max 0.5

However, the reusability and structural stability of the Na/CAC catalyst were not extensively examined in this study. Catalyst deactivation may occur due to Na leaching, surface fouling by glycerol, or pore blockage, which can reduce catalytic activity in repeated cycles. Therefore, future research should evaluate catalyst recovery, recyclability, and stability under multiple reaction cycles and continuous operation to assess its potential for industrial-scale biodiesel production.

Conclusion

This study successfully synthesized and applied the Na/CAC catalyst as a sustainable and low-cost heterogeneous catalyst for biodiesel production from UCO using ultrasound-assisted transesterification. The catalyst exhibited active sites of Na_2CO_3 and Na_2O, as confirmed by XRD, FTIR, SEM-EDX, and MAUD analyses, with a measured basicity of 7.71 mmol/g. The highest biodiesel yield of 73.15% was obtained under optimal conditions using 0.5% (wt%) catalyst loading and a 120-minute reaction time. The resulting biodiesel met the SNI 7182-2015 standard for fuel quality, and GC-MS analysis identified methyl oleate and methyl palmitate as the dominant FAME components. These findings demonstrate that Na/CAC is an efficient and environmentally friendly catalyst for biodiesel production from non-edible feedstocks, with ultrasonic assistance further improving reaction performance. Future studies should explore the catalyst's reusability and long-term stability and evaluate its performance in continuous or scaled-up production systems to validate its industrial applicability.

Acknowledgment

The authors express their sincere gratitude for the financial support provided by the Institute for Research and Community Service (LPPM) of Universitas Negeri Malang through Contract Number 24.2.651/UN32.14.1/LT/2025.

References

Al-Swaidan, H. M., & Ahmad, A. (2011). Synthesis and Characterization of Activated Carbon from Saudi Arabian Dates Tree's Fronds Wastes. *International Conference on Chemical, Biological and Environmental Engineering (IPCBEE)*, *20*. https://www.researchgate.net/publication/284662306_Synthesis_and_characterization_of_activated_carbon_from_Saudi_Arabian_dates_tree's_fronds_wastes

Ansori, A., & Mahfud, M. (2021). Ultrasound Assisted Interesterification for Biodiesel Production from Palm Oil and Methyl Acetate: Optimization Using RSM. *Journal of Physics: Conference Series*, *1747*(1). https://doi.org/10.1088/1742-6596/1747/1/012044

Chana, K., Chen, B. H., & Na-Ranong, D. (2025). Biodiesel Produced from Transesterification of Palm Oil Using NaOH-treated Activated Carbon and Pyrolytic Char of Used Tires as Catalysts. *Process Safety and Environmental Protection*, *195*, 1–13. https://doi.org/10.1016/j.psep.2025.01.004

Elgharbawy, A. S., Osman, A. I., El Demerdash, A. G. M., Sadik, W. A., Kasaby, M. A., & Ali, S. E. (2024). Enhancing Biodiesel Production Efficiency with Industrial Waste-Derived Catalysts: Techno-Economic Analysis of Microwave and Ultrasonic Transesterification Methods. *Energy Conversion and Management*, *321*, 1–12. https://doi.org/10.1016/j.enconman.2024.118945

Copyright © 2025 WJC | ISSN 2621-5985 (online) | ISSN 2549-385X (print)
Volume 8, Nomor 2, 2025

Gharby, S. (2022). Refining Vegetable Oils: Chemical and Physical Refining. *The Scientific World Journal*, *2022*(1), 1. https://doi.org/10.1155/2022/6627013

Helwani, Z., Negara, W. S., Zahrina, I., Amraini, S. Z., Idroes, G. M., Muslem, & Idroes, R. (2021). The Effect of KOH Concentration and Calcination Temperature on The Cement Clinker Catalyst Activity in The Transesterification of Off-Grade Palm Oil into Biodiesel. *IOP Conference Series: Materials Science and Engineering*, *1087*(1), 012061. https://doi.org/10.1088/1757-899X/1087/1/012061

Hendi, E. S., Rusdi, R., Alam, B. N., & Nurbaeti, S. (2021). Purification of Used Cooking Oil by Alkali Neutralization and Bleaching of Bayah Natural Zeolite. *Jurnal Bahan Alam Terbarukan*, *10*(1), 36–42. https://doi.org/10.15294/JBAT.V10I1.28636

Hisbullah, H. (2022). Characterization of Physically and Chemically Activated Carbon Derived from Palm Kernel. *International Journal of GEOMATE*, *23*(97), 203–210. https://doi.org/10.21660/2022.97.7554

Hoo, D. Y., Low, Z. L., Low, D. Y. S., Tang, S. Y., Manickam, S., Tan, K. W., & Ban, Z. H. (2022). Ultrasonic Cavitation: An Effective Cleaner and Greener Intensification Technology in the Extraction and Surface Modification of Nanocellulose. *Ultrasonics Sonochemistry*, *90*, 1–21. https://doi.org/10.1016/j.ultsonch.2022.106176

Kongto, P., Palamanit, A., Ninduangdee, P., Singh, Y., Chanakaewsomboon, I., Hayat, A., & Wae-hayee, M. (2022). Intensive Exploration of the Fuel Characteristics of Biomass and Biochar from Oil Palm Trunk and Oil Palm Fronds for Supporting Increasing Demand of Solid Biofuels in Thailand. *Energy Reports*, *8*, 5640–5652. https://doi.org/10.1016/J.EGYR.2022.04.033

Larimi, A., Harvey, A. P., Phan, A. N., Beshtar, M., Wilson, K., & Lee, A. F. (2024). Aspects of Reaction Engineering for Biodiesel Production. In *Catalysts* (Vol. 14, Issue 10). Multidisciplinary Digital Publishing Institute (MDPI). https://doi.org/10.3390/catal14100701

Mandari, V., & Devarai, S. K. (2022). Biodiesel Production Using Homogeneous, Heterogeneous, and Enzyme Catalysts via Transesterification and Esterification Reactions: a Critical Review. *Bioenergy Research*, *15*(2), 935–961. https://doi.org/10.1007/s12155-021-10333-w

Monika, Banga, S., & Pathak, V. V. (2023). Biodiesel Production from Waste Cooking Oil: A Comprehensive Review on the Application of Heterogenous Catalysts. *Energy Nexus*, *10*, 1–20. https://doi.org/10.1016/j.nexus.2023.100209

Naseef, H. H., & Tulaimat, R. H. (2025). Transesterification and Esterification for Biodiesel Production: A Comprehensive Review of Catalysts and Palm Oil Feedstocks. *Energy Conversion and Management: X*, *26*, 100931. https://doi.org/10.1016/J.ECMX.2025.100931

Nguyen, H. C., Nguyen, M. L., Su, C. H., Ong, H. C., Juan, H. Y., & Wu, S. J. (2021). Bio-derived catalysts: A Current Trend of Catalysts Used in Biodiesel Production. *Catalysts*, *11*(7), 1–28. https://doi.org/10.3390/catal11070812

Nyepetsi, M., Oyetunji, O. A., & Mbaiwa, F. (2024). Molecular Dynamics Study of the Thermodynamic Properties of Triglyceride/methanol Mixtures in the Presence of Cosolvent. *Journal of Molecular Liquids*, *399*, 1–15. https://doi.org/10.1016/J.MOLLIQ.2024.124431

Copyright © 2025 WJC | ISSN 2621-5985 (online) | ISSN 2549-385X (print)

Rahman, A., Oktaufik, M. A. M., Sasongko, T. W., Guntoro, I., Soedjati, D., Abbas, N., Rahman, A., Ulfah, F., Widiarto, A., Siswanto, Dharmawan, Trihadi, S. E. Y., Kusrestuwardani, Prihatin, A. L., Hadi, A., Indrijarso, S., Rahardjo, P., Barkah, A., Febijanto, I., & Sasongko, N. A. (2025). Current Scenario and Potential of Waste Cooking Oil as a Feedstock for Biodiesel Production in Indonesia: Life Cycle Sustainability Assessment (LCSA) Review. *Case Studies in Chemical and Environmental Engineering*, *11*, 101067. https://doi.org/10.1016/J.CSCEE.2024.101067

Siang, A. O. L., Leman, A. M., Feriyanto, D., Abdulmalik, S. S., & Zakaria, S. (2024). Sustainable Biodiesel Production from Waste Cooking Oil and Crude Palm Oil Using a Custom Mini Pilot Plant. *International Journal of Innovation in Mechanical Engineering and Advanced Materials*, *6*(1), 7–20. https://doi.org/10.22441/ijimeam.v6i1.23734

Suminar, D. R., Pribadi, C. Z., Fitriana, Q. R., Andrijanto, E., Permana, M. D., Eddy, D. R., & Rahayu, I. (2024). Corncob Waste Derived Carbon with Sulfonic Acid Group: An Efficient Heterogeneous Catalyst for Production of Ethyl Levulinate as Biodiesel Additives. *Heliyon*, *10*(18), 1–10. https://doi.org/10.1016/j.heliyon.2024.e37687

Tamilselvan, P., Sassykova, L., Prabhahar, M., Bhaskar, K., Kannayiram, G., Subramanian, S., & Prakash, S. (2020). Influence of Saturated Fatty Acid Material Composition in Biodiesel on its Performance in Internal Combustion Engines. *Materials Today: Proceedings*, *33*(1), 1181–1186. https://doi.org/10.1016/j.matpr.2020.07.626

Wang, S., Nam, H., Gebreegziabher, T. B., & Nam, H. (2020). Adsorption of acetic acid and hydrogen sulfide using NaOH impregnated activated carbon for indoor air purification. *Engineering Reports*, *2*(1). https://doi.org/10.1002/eng2.12083

Wirawan, S. S., Solikhah, M. D., Setiapraja, H., & Sugiyono, A. (2024). Biodiesel Implementation in Indonesia: Experiences and Future Perspectives. *Renewable and Sustainable Energy Reviews*, *189*, 113911. https://doi.org/10.1016/J.RSER.2023.113911

Copyright © 2025 WJC | ISSN 2621-5985 (online) | ISSN 2549-385X (print)